Optics & Laser Technology 199 (2026) 115076

Contents lists available at ScienceDirect

Optics and Laser Technology

journal homepage: www.elsevier.com/locate/optlastec

Full length article

# A 350-nm-band GaN/AlGaN multiple-quantum-well vertical cavity surface emitting laser

Yang Mei [a], Peng Gu [a], Rongbin Xu [a], Leiying Ying [a], Jing Yang [b], Degang Zhao [b], Feng Liang [b,*], Baoping Zhang [c,a,**]

[a] Laboratory of Micro/Nano-Optoelectronics, Department of Microelectronic and Integrated Circuits, Xiamen University, Xiamen 361005, China
[b] State Key Laboratory on Integrated Optoelectronics, Institute of Semiconductors, Chinese Academy of Sciences, Beijing 100083, China
[c] Institute of Nanoscience and Applications, Southern University of Science and Techonology,1088 Xueyuan Avenue, Shenzhen 518055, China

ARTICLE INFO

*Keywords:*
UVA VCSEL
GaN
Indium free
Low threshold

ABSTRACT

Optically pumped vertical-cavity surface-emitting lasers (VCSELs) operating in the 350 nm band were demonstrated. The VCSELs feature double dielectric distributed Brag reflectors and an AlGaN cavity, fabricated on Si (100) using the substrate transfer technique and laser lift-off. Indium-free GaN/$Al_{0.1}$GaN multi-quantum well (MQW) active region was used as the gain material. Optical property of the gain material was systemically studied by temperature and excitation power dependent photoluminescence measurement, and carrier localization effect was demonstrated in GaN/$Al_{0.1}$GaN MQWs. The shortest lasing wavelength of the fabricated VCSEL is ~356 nm, shorter than the band edge of GaN. The threshold pumping power density of the UVA VCSELs is ~0.8 MW/$cm^2$, which is among the lowest values for ultraviolet (UV) VCSELs. This study is promising for the development of small-footprint, power-efficient UV light sources.

## 1. Introduction

Semiconductor based ultraviolet (UV) lasers are of considerable interest for a wide variety of applications including chemical/biochemical analysis, high-density data storage, material processing, and laser lithography because of their high photon energy and the low diffraction limit of UV light [1–3]. They also hold great advantages of energy efficiency, stability, warming-up free, and compactness compared with conventional gas and solid-state UV lasers. As one typical type of semiconductor lasers, vertical cavity surface emitting lasers (VCSELs) are featured with low threshold operation, circular and low-divergence output beam, and low temperature sensitivity compared with those of edge-emitting laser diodes [4–8]. To date, GaAs-based VCSELs in near-infrared band have been successful in short-reach data communication since commercialization, and are further boosted by increasing demand for 3D sensing applications such as face recognition and autonomous driving. To shift the emission wavelength of the VCSELs shorter to visible and UV band, III-nitride based materials including InGaN, GaN, AlGaN, and AlN are ideal choices for their wide and tunable direct energy gaps (3.4 eV for GaN, and 6.0 eV for AlN) [9,10]. However, progress in developing UV VCSELs is still challenging when compared with their blue and green counterparts, and there is no electrically injected VCSEL with wavelength shorter than 400 nm. Even under the optical pumping excitation scheme, there are only very few reports, most of which are based on InGaN active layers with lasing wavelength longer than 363 nm or photon energy smaller than the band gap of GaN [11–18].

For UV VCSELs with InGaN active layers include small amounts of indium, emission efficiency is improved by the presence of indium-rich clusters, which allows the capture of electrons and holes in localized centers [1]. However, the inclusion of indium in the active layers inhibits emission at shorter UV wavelengths because of the very small bandgap of the InN and its sensitive growth condition. To further shift the emission wavelength to shorter UV wavelengths, indium free GaN or AlGaN active layers are needed, although the lack of indium in the active layers increases the probability of non-radiative recombination. Therefore, it is important to grow the indium free active layers with high crystal quality to guarantee the emission efficiency without the

* Corresponding author.
** Corresponding author at: Laboratory of Micro/Nano-Optoelectronics, Department of Microelectronic and Integrated Circuits, Xiamen University, Xiamen 361005, China.
*E-mail addresses:* liangfeng13@semi.ac.cn (F. Liang), bzhang@xmu.edu.cn (B. Zhang).

https://doi.org/10.1016/j.optlastec.2026.115076
Received 14 January 2025; Received in revised form 20 December 2025; Accepted 3 March 2026
Available online 7 March 2026

assistance of indium. Early in 1996, Redwing et al. have ever fabricated UVA VCSELs with $Al_{0.40}Ga_{0.60}N/Al_{0.12}Ga_{0.88}N$ DBRs, and a 10 μm thick indium free bulk GaN was used as the active layer [19]. Optically pumped lasing at 363 nm was realized with a threshold of ~ 2 $MW/cm^2$. In 2018, Lu et al. also reported UVA VCSELs with a 3.8 μm thick bulk GaN active layer [20]. $TiO_2$ based high-contrast grating (HCG) was fabricated as the top mirror, and lasing at 369.1 nm was realized. However, emission wavelength of bulk GaN is limited by the bandgap and the differential gain is low when compared with the quantum structures such as the QWs and quantum dots [21]. In 2020, by growing $Al_{0.2}GaN/Al_{0.5}GaN$ MQWs with high crystal quality and fabricating a dual dielectric DBR cavity with low loss, Hjort et al. reported the first UVB VCSELs lasing at 310 nm [22,23]. In our previous work, we also successfully fabricated the first UVC VCSEL lasing at 275.9 nm by using $Al_{0.4}GaN/Al_{0.5}GaN$ MQW active region [3]. But for the VCSELs emitting in UVA band (320 nm-400 nm) which is important for applications including UV curing, light therapy, air purification, and 3D printing, there is still no report of devices with lasing wavelength shorter than the band edge of GaN.

In this study, we demonstrate the 350-nm-band UVA VCSELs based on indium free $GaN/Al_{0.1}GaN$ MQW active region and a dual dielectric DBR cavity. The epi-structure was grown on sapphire substrate and then transferred to Si (100) substrate. Optically pumped lasing at 356 nm was demonstrated at room temperature with a threshold excitation power density of 0.8 $MW/cm^2$.

## 2. Materials and methods

The epitaxial wafer used in this study was grown on a sapphire substrate by using the MOCVD system. The epi-structure as well as the fabrication process of the VCSEL are shown schematically in Fig. 1. The UVA VCSEL consists of a ~1 μm thick AlGaN cavity including two GaN QWs, sandwiched between a top 8.5-pair and bottom 12.5-pair dielectric $HfO_2/SiO_2$ DBRs with reflectivity >99%. To realize the VCSEL structure, the bottom DBR was first deposited on the surface of the epitaxial wafer by e-beam evaporation. The wafer was then flip-chip adhesive bonded to a Si (100) substrate, and the sapphire substrate was removed by laser lift-off (LLO). The flip-chip bonding process was conducted by using a kind of UV-curable adhesive NOV61 purchased from Norland Products, INC. The wafer was simply placed on Si substrate after spin coating of adhesive, and the adhesive bonding material was then cured under a UV LED lamp (365 nm) for 20 min. No additional heating or pressurization was required during the bonding process. The LLO process was performed using a pulsed 248-nm KrF excimer laser with pulse width ~1 ns, and the laser energy density (~2.7 $J/cm^2$) as well as the laser spot size (1.5*1 $mm^2$) were optimized to avoid the damage to the epi-layers. After LLO, chemical mechanical polishing (CMP) was used to obtain a flat cavity surface and thin the epi-layer, and the root-mean-square roughness of the surface after CMP is ~0.19 nm on a 5 × 5 $μm^2$ area. The flat cavity surface is essential to reduce the scattering loss, which is important for the realization of low threshold lasing. Finally, the top DBR was deposited to complete the optically pumped UVA VCSEL structure. The detailed fabrication processes are similar with our previous reports [3,18].

## 3. Results and discussion

The emission spectra of the epitaxial wafers and the UVA VCSELs were measured under excitation by a 320 nm pulsed laser with a repetition frequency of 20 Hz and a pulse width of 5 ns. Excitation laser was focused on the surface of the sample with a microscope objective (40 × NUV), and the diameter of the excitation spot was ~160 μm. Then the light was guided through air into a monochromator with an electrically cooled charge-coupled device (CCD) as the detector. Fig. 2 shows the temperature dependent photoluminescence (PL) spectra of the epi-wafer. Under low temperature of 3 K, the PL spectrum exhibits 2 narrows peaks centered at 3.566 and 3.510 eV, which are defined as Peak 1 and Peak 2, respectively. With increasing temperature, both the two peaks broaden and emerge together. Peaks 1 shows a slight redshift first when temperature increased from 3 K to 10 K, and then exhibits blueshift from 3.564 to 3.568 eV in the temperature range from 10 to 50 K. In the temperature range from 50 to 300 K, Peak 1 shows a red shift to 3.48 eV with increasing temperature. Differently, Peak 2 shows a monotonically redshift from 3.510 to 3.395 eV when temperature increased from 3 to 300 K. The photon energy evolution of Peak 1 and 2 are shown in Fig. 2. The origin of Peak 2 can be explained by the emission from the GaN template in the epi-structure, since the peak energies under 3 K and room temperature of Peak 2 consist well with that of bulk GaN [24]. The monotonically redshift of Peak 2 is caused by the thermal quenching of band gap. The emission of Peak 1 can be deduced from the emission of GaN MQWs, and the slight "S" behavior demonstrates the existence of slight carrier potential localization effect although without Indium,

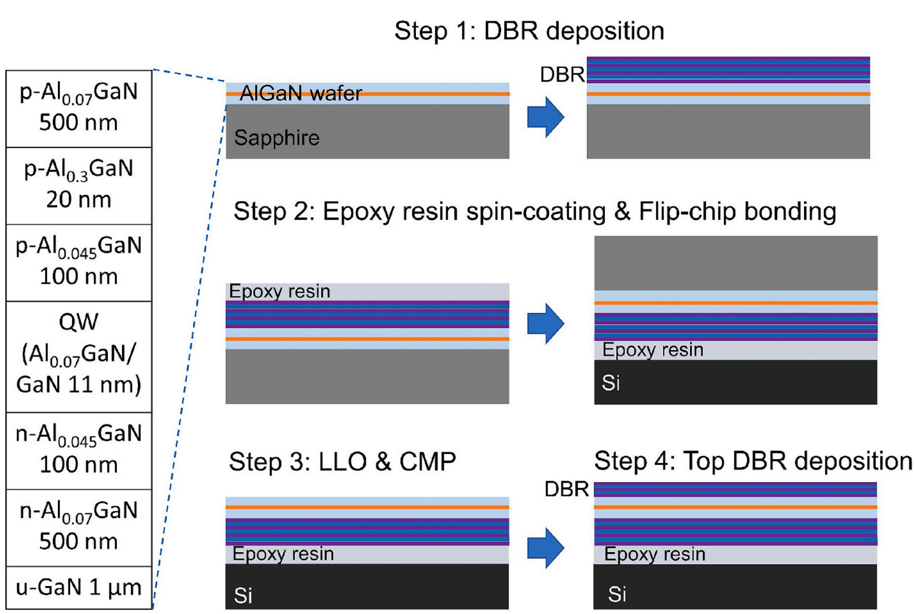


**Fig. 1.** Epi-structure and device fabrication processes of the UVA VCSEL.

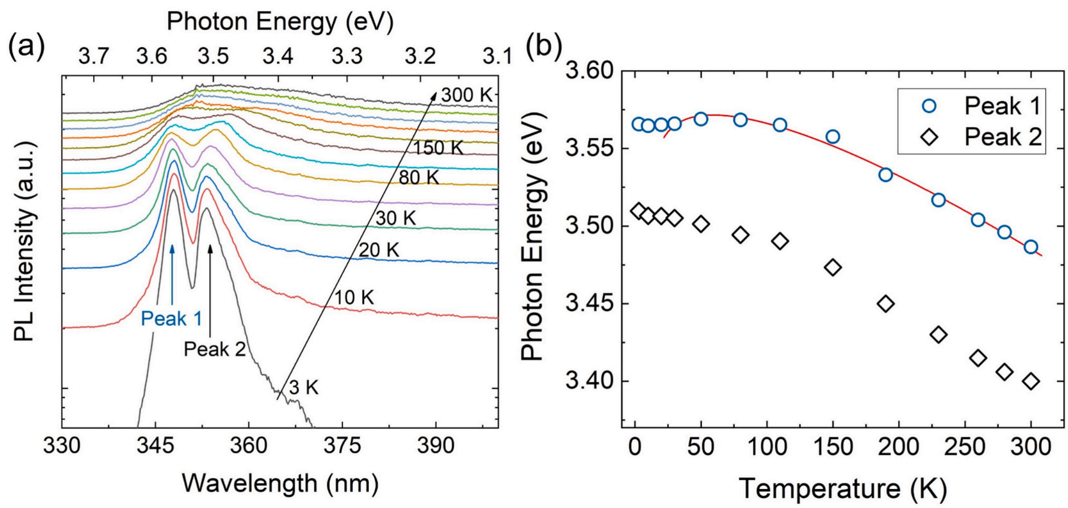


**Fig. 2.** (a) Temperature dependent PL spectra of the epi-wafer. (b) Photon energy evolution of the epi-wafer under different temperature.

which is common and more pronounce in InGaN QWs caused by indium content fluctuation. The photon energy of Peak 1 as a function of temperature is fitted by the widely used Varshni's empirical formula [25,26]:

$$E_g(T) = E_g(0) - \left(\frac{\alpha T^2}{\beta + T}\right) - \frac{\sigma^2}{k_B T} \tag{1}$$

where $E_g(0)$ is the band-gap energy at T = 0 K, α and β are Varshni's thermal coefficients, σ is the standard deviation of the energy distribution width of localized states, and kB is the Boltzmann constant. The solid red lines in Fig. 2b are the fitting curves according to Eq. (1). The parameters α and β were set to 0.43 meV $K^{-1}$ and 650 K, respectively. The fitted σ value, which indicates the degree of localization effect and broadening of the spectra, was 6 meV, similar with previous study [27]. The σ is much smaller than the typical values of several tens meV in InGaN QWs, and the slight carrier localization effect here can be caused by the inhomogeneous strain and thickness of the GaN QWs [28]. The excitation energy dependent PL spectra of the epi-wafer were also measured at room temperature, as shown in Fig. 3 a. The spectra are plotted in log scale and the two peaks from GaN template and GaN QWs can still be distinguished at room temperature. The photon energy of Peak 1 is almost fixed with increasing excitation energy. For InGaN QWs with high Indium content and localization effect, the excitation energy dependent emission wavelength typically shows a blue shift followed by red shift caused by carrier screening and band filling effect. The stable emission of GaN based MQWs here is favorable for laser fabrication due to the stable gain spectrum under different excitation levels.

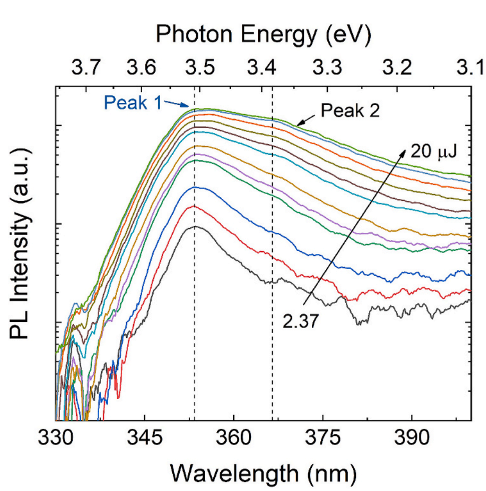


**Fig. 3.** Excitation energy dependent PL spectra of the epi-wafer.

During device fabrication, the excitation power density dependent PL spectra of the sample before the deposition of the top DBR, which is defined as the half-cavity device, were also measured and exhibit very different behavior from the as-grown epi-wafer. With increasing excitation power density, the linewidth of the spontaneous spectrum exhibited a sudden decrease, and a peak with a linewidth of 3 nm emerged at 354.8 nm, as shown in Fig. 4 a. The integrated intensity of the whole spectrum and the corresponding linewidth under different excitation power density are shown in Fig. 4 b. The clear threshold and spectral narrowing reflect the onset of the stimulated emission in the sample with half-cavity at room temperature. This demonstrates the high material gain and the potential to develop UVA VCSELs in the 350 nm band.

After fabrication of the full cavity structure, the VCSEL's optical emission spectra at room temperature for different pump levels were measured, as shown in Fig. 5 a. Multi sharp peaks near ~356 nm can be observed with increasing excitation energy, which can be explained by the multi-mode lasing. Such multimode emission in optically pumped VCSELs usually comes from the different lasing spots in the excitation area, and similar phenomenon has also been reported in other UV VCSELs [23]. Fig. 5 b shows emission intensity as well as the spectral linewidth as a function of the excitation power density. The emission intensity is calculated by integrating over the entire multimode spectrum. A clear lasing threshold and spectral narrowing happens around 0.8 $MW/cm^2$. The threshold is also among the typical values of the reported UV VCSELs. The threshold carrier density inside the active region was calculated to be ~9 e19 $cm^{-3}$ following the rate equation model [29,30]. And this is larger than that of visible InGaN based VCSELs [31], which is mainly caused by the higher cavity loss and smaller material gain in UV spectral region. The linewidth of the VCSEL decreased from 10 nm to 1 nm when the lasing threshold was reached. Note that the relatively broad linewidth of ~1 nm after lasing was extracted from the whole lasing spectrum, and this is caused by the overlapping of the multi-peaks with small mode spacing.

Due to the slight cavity thickness fluctuation caused by the CMP process, different lasing behavior can also be observed from the sample when we pump at different area. Fig. 6 a shows the excitation power density dependent spectra of a lasing spot which exhibit lasing at ~358 nm. Several tiny modes belong the main peak with very small mode spacing can be distinguished, and they compete with each other during the variation of the excitation power. The mode competition is also an

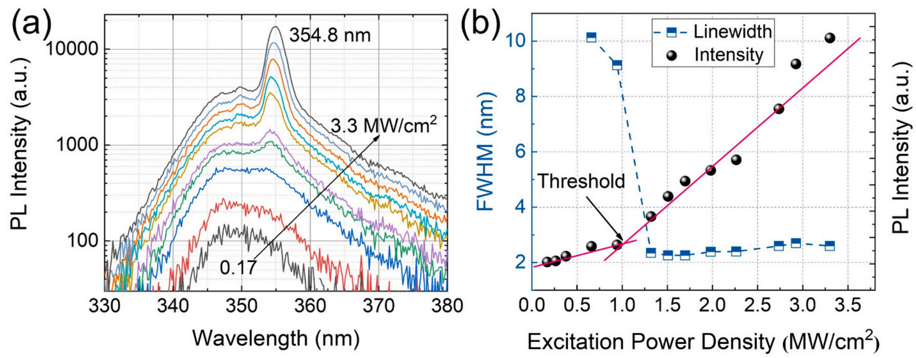


**Fig. 4.** (a) Excitation energy dependent PL spectra of the half-cavity device. (b) Intensity and linewidth of the device as a function of excitation energy.

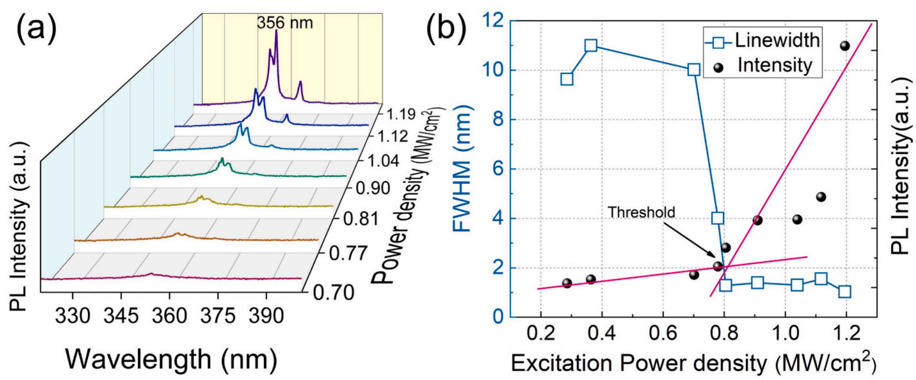


**Fig. 5.** (a) Excitation energy dependent PL spectra of the VCSEL lasing at 356 nm. (b) Intensity and linewidth of the device as a function of excitation power density.

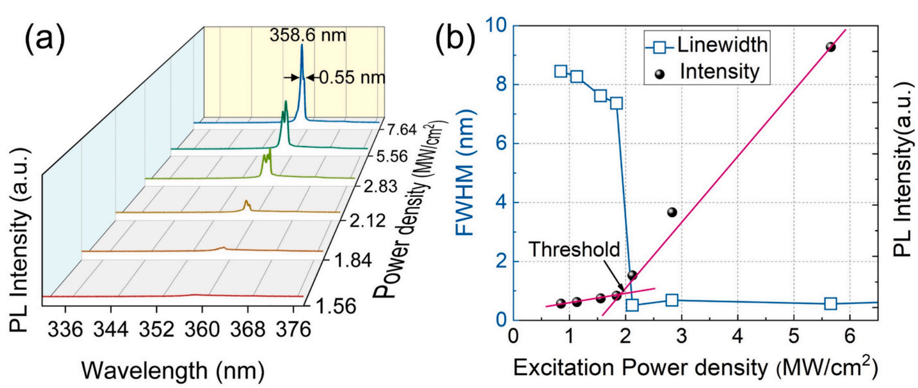


**Fig. 6.** (a) Excitation power density dependent PL spectra of the VCSEL lasing at 358.6 nm. (b) Intensity and linewidth of the device as a function of excitation energy.

evidence of the onset of lasing action. The integrated intensity of all the tiny modes and the linewidth of the spectra as a function of excitation power density is given in Fig. 6 b, from which a clear threshold can be obtained at ~ 2 MW/cm$^2$. To further prove the lasing action in the UV VCSEL, the polarization characteristic of the device was measured, as shown in Fig. 7. The polarization ratio is relatively high to be ~87%, which is among the typical values of GaN based VCSELs after lasing. The high-resolution spectrum of the device under excitation power density of 2.83 MW/cm$^2$ is given in Fig. 8, showing three modes with spacing of ~0.6 nm. The linewidth of the mode Peak 1 with the lowest emission energy is ~0.22 nm determined by Lorentzian fitting, which is near the resolution limit of the spectrometer used in this study. And the Q factor was calculated to be ~1497.5. Peak 2 and 3 show a larger linewidth with increasing emission energy, corresponding to Q factor of 608 and 550, respectively. This is a typical phenomenon of lateral confined optical modes in VCSELs, and the mode Peak 1 with longest wavelength is the fundamental mode, while Peak 2 and 3 are high order lateral modes. High order lateral modes usually have larger optical losses, therefore a smaller Q factor. The excitation induced higher temperature can increase the refractive index of the lasing spot, thus inducing the lateral optical confinement and the generation of the high order lateral modes for optically pumped VCSELs [32].

The lasing wavelength as well as threshold of the ever-reported UVA VCSELs were collected in Fig. 9 for comparation with the results in this study. Note that the UVB VCSEL [23] and UVC VCSEL [3] reported in our previous work are not collected because this study mainly concentrates on devices in UVA band. The device in this study can realize shorter lasing wavelength beyond the band-edge of GaN, while maintaining the comparable threshold with that of devices using InGaN active regions.

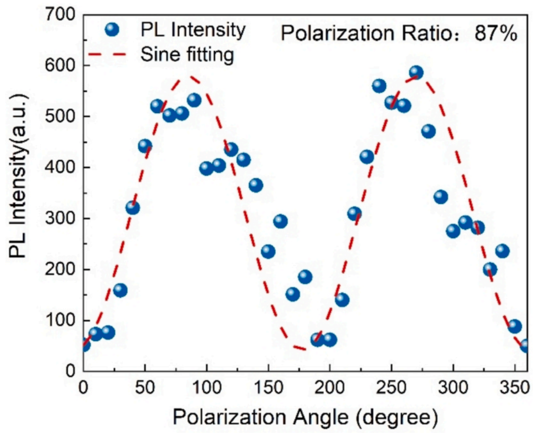


**Fig.7.** Polarization characteristic of the UVA VCSEL.

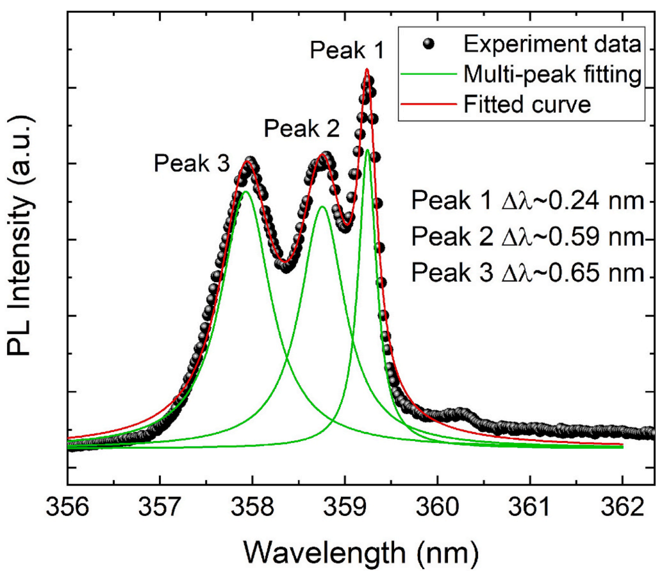


**Fig. 8.** High-resolution spectrum and multi-peak fitting of the VCSEL under excitation power density of 2.83 MW/cm$^2$.

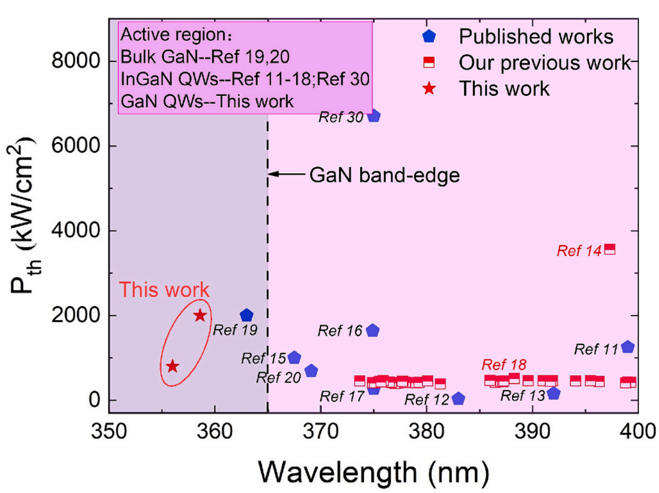


**Fig. 9.** Lasing threshold and wavelength of the reported UVA VCSELs and results in this study [11–20,33].

## 4. Conclusion

In summary, the 350-nm-band GaN/AlGaN MQW VCSEL on Si (100) has been demonstrated under optically pumped condition at room temperature. The shortest lasing wavelength is 356 nm, beyond the band edge of GaN, and the lasing threshold is 0.8 MW/cm$^2$. This study is promising for the development of GaN-based UVA laser sources, and electrically injected UVA VCSELs can be expected in near future by improving material quality and device design.

## CRediT authorship contribution statement

**Yang Mei:** Writing – review & editing, Writing – original draft, Methodology, Formal analysis, Data curation, Conceptualization. **Peng Gu:** Methodology, Investigation, Data curation. **Rongbin Xu:** Methodology. **Leiying Ying:** Methodology. **Jing Yang:** Methodology. **Degang Zhao:** Resources, Investigation. **Feng Liang:** Methodology. **Baoping Zhang:** Conceptualization.

## Funding

This work was supported by Natural Science Foundation of Fujian Province (NO. 2023J05020); National Natural Science Foundation of China (No. 62474150, U21A20493, 62234011); National Key Research and Development Program of China (2024YFB3613100); Natural Science Foundation of Gaungdong Province (2025A1515011349).

## Declaration of competing interest

The authors declare that they have no known competing financial interests or personal relationships that could have appeared to influence the work reported in this paper.

## Data availability

Data underlying the results presented in this paper are not publicly available at this time but may be obtained from the authors upon reasonable request.

## References

[1] H. Yoshida, Y. Yamashita, M. Kuwabara, H. Kan, A 342-nm ultraviolet AlGaN multiple-quantum-well laser diode, Nat. Photonics 2 (9) (2008) 551–554.
[2] Z. Zhang, et al., A 271.8 nm deep-ultraviolet laser diode for room temperature operation, Appl. Phys Express 12 (12) (2019) 124003.
[3] Z. Zheng, et al., AlGaN-based deep ultraviolet vertical-cavity surface-emitting laser, IEEE Electron Device Lett. 42 (3) (2021) 375–378.
[4] T. Hamaguchi, GaN-based VCSELs with a monolithic curved mirror: challenges and prospects, Photonics 10 (4) (2023) 470.
[5] Y. Mei, et al., Quantum dot vertical-cavity surface-emitting lasers covering the 'green gap', Light Sci. Appl. 6 (1) (2017) e16199.
[6] H.-C. Yu, et al., Progress and prospects of GaN-based VCSEL from near UV to green emission, Prog. Quantum Electron. 57 (2018) 1–19.
[7] K. Iga, Forty years of vertical-cavity surface-emitting laser: invention and innovation, Jpn. J. Appl. Phys. 57 (8S2) (2018) 08PA01.
[8] K. Iga, "VCSEL: born small and grown big," in Vertical External Cavity Surface Emitting Lasers *(VECSELs)* X, 2020, vol. 11263: SPIE, p. 1126302.
[9] H.A.A.A. Amir, M.A. Fakhri, A.A. Alwahib, Review of GaN optical device characteristics, applications, and optical analysis technology, Mater. Today Proc. 42 (2021) 2815–2821.
[10] Y. Chen, et al., Review on the progress of AlGaN-based ultraviolet light-emitting diodes, Fundam. Res. 1 (6) (2021) 717–734.
[11] T. Someya, R. Werner, A. Forchel, M. Catalano, R. Cingolani, Y. Arakawa, Room temperature lasing at blue wavelengths in gallium nitride microcavities, Science 285 (5435) (1999) 1905–1906.
[12] H. Zhou, et al., Near ultraviolet optically pumped vertical cavity laser, Electron. Lett 36 (21) (2000) 1777–1779.
[13] S.-H. Park, et al., Room-temperature GaN vertical-cavity surface-emitting laser operation in an extended cavity scheme, Appl. Phys. Lett. 83 (11) (2003) 2121–2123.
[14] J.-Y. Zhang, et al., Blue-violet lasing of optically pumped GaN-based vertical cavity surface-emitting laser with dielectric distributed Bragg reflectors, J. Lightwave Technol. 27 (1) (2009) 55–59.

[15] Y.-S. Liu *et al.*, Development for ultraviolet vertical cavity surface emitting lasers, in The European Conference on Lasers and Electro-Optics, 2015: Optica Publishing Group, p. PD_A_2.

[16] Y.-S. Liu, et al., Optically pumped vertical-cavity surface-emitting laser at 374.9 nm with an electrically conducting n-type distributed Bragg reflector, Appl. Phys Express 9 (11) (2016) 111002.

[17] Y. J. Park *et al.*, "Optically pumped vertical-cavity surface-emitting lasers at 375 nm with air-gap/Al0. 05Ga0. 95N distributed Bragg reflectors," in *Vertical-Cavity Surface-Emitting Lasers XXIII*, 2019, vol. 10938: SPIE, pp. 27-33.

[18] Y. Mei, et al., Low-threshold wavelength-tunable ultraviolet vertical-cavity surface-emitting lasers from 376 to 409 nm, Fundam. Res. 1 (6) (2021) 684–690.

[19] J.M. Redwing, D.A. Loeber, N.G. Anderson, M.A. Tischler, J.S. Flynn, An optically pumped GaN–AlGaN vertical cavity surface emitting laser, Appl. Phys. Lett. 69 (1) (1996) 1–3.

[20] T.-C. Chang, S.-Y. Kuo, E. Hashemi, Å. Haglund, T.-C. Lu, GaN vertical-cavity surface-emitting laser with a high-contrast grating reflector, High Contrast Metastructures VII 10542 (2018) 30–35.

[21] D. Bimberg, N. Ledentsov, Quantum dots: lasers and amplifiers, J. Phys. Condens. Matter 15 (24) (2003) R1063.

[22] G. Cardinali *et al.*, "Low-threshold AlGaN-based UVB VCSELs enabled by post-growth cavity detuning," *Applied Physics Letters,* vol. 121, no. 10, 2022.

[23] F. Hjort, et al., A 310 nm optically pumped AlGaN vertical-cavity surface-emitting laser, ACS Photon. 8 (1) (2020) 135–141.

[24] T. Hanada, Basic properties of ZnO, GaN, and related materials, in: Oxide and Nitride Semiconductors: Processing, Properties, and Applications, Springer, 2009, pp. 1–19.

[25] A. Tian, et al., Optical characterization of InGaN/GaN quantum well active region of green laser diodes, Appl. Phys Express 10 (1) (2016) 012701.

[26] L. Zhu, B. Liu, Optical properties studies in InGaN/GaN multiple-quantum well, Solid State Electron. 53 (3) (2009) 336–340.

[27] P. Eliseev, The red σ2/kT spectral shift in partially disordered semiconductors, J. Appl. Phys. 93 (9) (2003) 5404–5415.

[28] J. Mickevičius, et al., Influence of carrier localization on high-carrier-density effects in AlGaN quantum wells, Opt. Express 22 (102) (2014) A491.

[29] T. Baba, D. Sano, Low-threshold lasing and Purcell effect in microdisk lasers at room temperature, IEEE J. Sel. Top. Quantum Electron. 9 (5) (2004) 1340–1346.

[30] F. Tabataba-Vakili *et al.*, Analysis of low-threshold optically pumped III-nitride microdisk lasers, Appl. Phys. Lett., 117, 12, 2020.

[31] Y.C. Wang, T. Yang, L. Shi, Y.-H. Chen, Y. Mei, B.-P. Zhang, Simulation of performance enhancement of GaN-based VCSELs by composition gradient InGaN last-quantum barrier, Semicond. Sci. Technol. 38 (12) (2023) 125003.

[32] S. Anguiano, A.A. Reynoso, A.E. Bruchhausen, A. Lemaitre, J. Bloch, A. Fainstein, Three-dimensional trapping of light with light in semiconductor planar microcavities, Phys. Rev. B 99 (19) (2019) 195308.

[33] C. Zhang, R. T. ElAfandy, J. Zhang, S. Chen, A. Nurmikko, and J. Han, "Development of nanopore-based near ultraviolet vertical-cavity surface emitting lasers," in Gallium Nitride Materials and Devices XIV, 2019, 10918: SPIE, 138–148.